Reactive dynamics of inertial particles in nonhyperbolic chaotic flows

Adilson E. Motter,[1,*] Ying-Cheng Lai,[2] and Celso Grebogi[3]
[1]*Max Planck Institute for the Physics of Complex Systems, Nöthnitzer Strasse 38, 01187 Dresden, Germany*
[2]*Departments of Mathematics, Electrical Engineering, and Physics, Arizona State University, Tempe, Arizona 85287, USA*
[3]*Instituto de Física, Universidade de São Paulo, Caixa Postal 66318, 05315-970 São Paulo, Brazil*
(Received 23 April 2003; published 20 November 2003)

Anomalous kinetics of infective (e.g., autocatalytic) reactions in open, nonhyperbolic chaotic flows are important for many applications in biological, chemical, and environmental sciences. We present a scaling theory for the singular enhancement of the production caused by the universal, underlying fractal patterns. The key dynamical invariant quantities are the *effective fractal dimension* and *effective escape rate*, which are primarily determined by the hyperbolic components of the underlying dynamical invariant sets. The theory is general as it includes all previously studied hyperbolic reactive dynamics as a special case. We introduce a class of dissipative embedding maps for numerical verification.

DOI: 10.1103/PhysRevE.68.056307 PACS number(s): 47.70.Fw, 05.45.−a, 47.52.+j, 47.53.+n

Many chemical and biological processes in fluids are characterized by a filamental distribution of active particles along fractal invariant sets of the advection chaotic dynamics. These fractal structures act as dynamical catalysts for the reaction, which is relevant for a variety of environmental processes in open flows, such as ozone depletion in the atmosphere [1] and population dynamics of plankton in the oceans [2].

The study of active processes in open chaotic flows has attracted a great deal of interest from the dynamical system community [3,4]. Most of the studies have been performed for time-dependent two-dimensional incompressible flows, in the limit of weak diffusion. The flow is nonturbulent, but the particle dynamics is considered to be chaotic (Lagrangian chaos) and the active particles to interact with one another without modifying the flow. The advection dynamics of such particles can be cast in the context of chaotic scattering, where incoming tracers spend some time in a mixing (scattering) region before being scattered along the unstable manifold of the chaotic saddle. As a result, the products of the reaction concentrate along a fattened-up copy of the unstable manifold, giving rise to the observed fractal patterns.

Although filamental patterns have been observed in nature, a clear relation between the observed value of the fractal dimension and the underlying advection dynamics has been lacking. For example, in the "flow past a cylinder" system previously considered [3], the dimension of the unstable manifold is known to be 2 but the relevant dimension governing infective and collisional reactions is about 1.6. This lack of relation, while not reducing the importance of the previous phenomenological characterization of filamental distributions of active particles, has led to some skepticism about the merit of the dynamical system approach to the problem. In general, the advection dynamics can be characterized as either hyperbolic or nonhyperbolic. In hyperbolic chaotic scattering, all the periodic orbits are unstable and there are no Kolmogorov-Arnold-Moser (KAM) tori in the phase space, while the nonhyperbolic counterpart is frequently characterized as having both chaotic and marginally stable periodic orbits. Fundamental assumptions in such works are that (1) the active particles are massless pointlike tracers and (2) the advection dynamics of these particles is hyperbolic [5]. However, in realistic situations, the Lagrangian dynamics is typically nonhyperbolic and the active particles have finite size and inertia. Indeed, fully hyperbolic systems are quite rare and represent very idealized situations as the advection dynamics of tracers in fluids is usually constrained to have a nonhyperbolic character because of no-slip boundary conditions at the surface of obstacles. Obstacles are at the same time the origin of Lagrangian chaos and the origin of nonhyperbolicity. Even away from obstacles and boundaries, chaotic motions of tracers typically coexist with regular motions. In addition, the individual active particles are often too large to be regarded as noninertial, as is the case for many species of zooplankton in the sea. Therefore, nonhyperbolic and inertial effects are prevalent in nature and expected to play an important role in most environmental processes. A question of physical importance is then: What happens to the reactive dynamics when assumptions (1) and (2) are dropped?

In this article, we present a scaling theory for the reactive dynamics of inertial particles in nonhyperbolic chaotic flows. The key concepts in our framework are the *effective fractal dimension* and *effective escape rate*, which are respectively defined as

$$D_{eff}(\varepsilon)=-\frac{d\ln N(\varepsilon)}{d\ln\varepsilon}, \tag{1}$$

$$\kappa_{eff}(\varepsilon)=-\frac{d\ln R(n)}{dn}, \tag{2}$$

where $N(\varepsilon)$ is the number of ε-squares needed to cover the relevant fractal set, and $R(n)$ is the fraction of particles that takes more than $n=n(\varepsilon)$ steps to escape from the mixing region (see below). As a representative application of these concepts, we show, for autocatalytic reactions of the form

*Electronic address: motter@mpipks-dresden.mpg.de

$A+B\rightarrow 2B$, that the area covered by B particles in the steady state obeys the following scaling law:

$$\mathcal{A}_B \sim \left[\frac{\sigma}{e^{\mu_{eff}/(2-D_{eff})}-1} \right]^{2-D_{eff}}, \quad (3)$$

where $\mu_{eff} \equiv (\kappa_{eff}+\tilde{\kappa})\tau$, τ is the time interval between successive reactions (time lag), σ is the reaction range, and $\tilde{\kappa}$ is the contraction rate due to dissipation. For nonhyperbolic flows in two dimensions, $D_{eff}<2$ and $\kappa_{eff}>0$ are nontrivial functions of the scale ε, which can often be regarded as constants over a wide interval, even though $D = \lim_{\varepsilon\rightarrow 0} D_{eff}(\varepsilon)=2$ and $\kappa = \lim_{\varepsilon\rightarrow 0}\kappa_{eff}(\varepsilon)=0$. We find, surprisingly, that D_{eff} and κ_{eff} are significantly different from D and κ, respectively, not only for noninertial but also for inertial particles, even though the advection dynamics of the latter is hyperbolic, meaning that *scars* of the nonhyperbolic conservative dynamics are observable in the hyperbolic dynamics of slightly dissipative systems ($\tilde{\kappa} \ll 1$). The previous relations for noninertial particles in hyperbolic fluids appear as a particular case of our results.

The nature of the chaotic scattering arising in the context of particle advection in incompressible fluids may change fundamentally as the mass and size of the particles are increased from zero. Physically, this happens because of the detachment of the particle motion from the local fluid motion. For spherical particles of finite size, the particle velocity $\mathbf{v} \equiv d\mathbf{x}/dt$ is typically different from the (time-dependent) fluid velocity $\mathbf{u}=\mathbf{u}(\mathbf{x},t)$ and, in first order, is governed by the equation [6]

$$\frac{d\mathbf{v}}{dt} - \alpha \frac{d\mathbf{u}}{dt} = -a(\mathbf{v}-\mathbf{u}). \quad (4)$$

The parameters are $\alpha = 3\rho_f/(\rho_f+2\rho_p)$ and $a=\frac{2}{3}\alpha/\mathrm{St}$, where ρ_f and ρ_p are the densities of fluid and particle, respectively, and St is the Stokes number, which goes to zero in the limit of pointlike particles [7]. For neutrally buoyant particles, the mass ratio parameter is $\alpha=1$, while for aerosols and bubbles we have $\alpha<1$ and $\alpha>1$, respectively. The inertia parameter a determines the contraction rate or dissipation in the *phase space* $(\mathbf{x},\mathbf{v})$, which for incompressible flows can be shown to be $-2a$. In the limit $a\rightarrow\infty$, the dynamics is projected on a surface defined by $\mathbf{v}=\mathbf{u}$, which corresponds to the advection dynamics of point particles. The *configuration-space* projection of the particle motion is strongly influenced by α [8]. For small inertia (large a), $\nabla\cdot\mathbf{v} \approx a^{-1}(\alpha-1)\nabla\cdot[(\mathbf{v}\cdot\nabla)\mathbf{u}] = a^{-1}(\alpha-1)(s^2-\omega^2)$, where s and ω are proportional to the strain rate and vorticity of the fluid [9], respectively. The behaviors of bubbles and aerosols are then qualitatively different. For instance, along a closed orbit, aerosols are pushed outward, while bubbles are pushed inward. We first consider bubbles, whose configuration-space dynamics is dissipative when the vorticity overcomes the strain rate.

Dynamically, the inertial effects are effectively those due to dissipation, so that the transition to finite inertia is equivalent to a transition from open Hamiltonian to dissipative dynamics. It has been recently shown [10] that, while hyperbolic dynamics is robust, nonhyperbolic chaotic scattering typically undergoes a metamorphosis in the presence of arbitrarily small amount of dissipation. For nonhyperbolic scattering in open Hamiltonian systems, particles can spend a long time in the neighborhood of KAM tori, resulting in an algebraic decay for the survival probability of particles in the scattering region. As a consequence, the fractal dimension of the invariant manifolds is the phase-space dimension [11]. This should be contrasted with the hyperbolic case, whose decay is exponential and fractal dimension is typically smaller. The dissipation, however, may convert marginally stable periodic orbits of the KAM islands into attractors. The survival probability then becomes exponential, the dimension of the chaotic saddle becomes fractional, and the overall dynamics of the scattering process becomes hyperbolic.

To understand the meanings of D_{eff} and κ_{eff} for fractal sets arising in the transition from Hamiltonian nonhyperbolic to weakly dissipative chaotic scattering, we consider a Cantor set, which is constructed in the interval $[0,1]$ according to the rule that in the nth time step, a fraction $\Delta_n = \gamma/(\beta+n)+\delta$ is removed from the middle of each one of the $N=2^{n-1}$ remaining subintervals, where β, γ, and δ are constants. The conservative case corresponds to $\delta=0$, which is characterized by an algebraic decay with n of the total length remaining, given by $R(n)\sim n^{-\gamma}$ for $n\gg\beta$, and by a unity fractal dimension for the invariant set, $D=1$. The removed fraction Δ_n decreases at each time step and, as a result, a systematic change of scales is induced, resulting in a non-self-similar invariant set that becomes denser as we go to smaller scales. The relevant consequence is that the box-counting dimension converges slowly to 1, leading to a scale-dependent effective fractal dimension $D_{eff}\approx 1-\gamma/\ln\varepsilon^{-1}$ for small ε. Similarly, the effective escape rate behaves as $\kappa_{eff}\approx\gamma/n\approx\gamma\ln 2/\ln\varepsilon^{-1}$, where $n=n(\varepsilon)$ is defined as the number of iterations needed to make the length of each remaining subinterval smaller than ε.

The limiting dynamics changes drastically and acquires properties of hyperbolic dynamics when a small amount of dissipation is allowed, which is modeled by $0<\delta\ll\gamma/\beta$. In particular, the total length of the remaining intervals decays exponentially, $R(n)\sim(1-\delta)^n$ for $n\gg\gamma/\delta-\beta$, and the dimension of the invariant set becomes smaller than 1, namely, $D=\ln 2/\ln[2/(1-\delta)]$. At finite time, however, the transition from the conservative to the dissipative case is much smoother. For $\ln\varepsilon^{-1}\gg\beta$, the effective fractal dimension and the effective escape rate are $D_{eff}(\varepsilon)\approx\ln 2/\ln[2/(1-\delta)]-\gamma'/\ln\varepsilon^{-1}$ and $\kappa_{eff}(\varepsilon)\approx\ln(1-\delta)^{-1}+\gamma'\ln[2/(1-\delta)]/\ln\varepsilon^{-1}$, respectively, where $\gamma'\equiv\gamma/(1-\delta)$. The key feature is that unrealistically small scales are required to resolve the limiting values of the fractal dimension and the escape rate, rendering them physically irrelevant. For instance, to obtain $D_{eff}>0.95$, scales $\varepsilon<10^{-20}$ may be required. Thus, the physically important characteristics of the fractal set are the effective dimension and escape rate.

We now present a physical theory for the scaling law (3), valid for autocatalytic reactions in two-dimensional time-periodic flows. Consider the area covered by B particles in the open part of the flow (i.e., region where particles eventually escape to infinity) and, to be specific, that the time lag τ is integer multiple of the flow's period. After a sufficiently long time from the onset of the reaction, the reagent B is distributed along stripes of approximately uniform width, mimicking the unstable manifold. The average width ϵ of the stripes changes aperiodically over time until the steady state is reached, when it undertakes the periodicity τ of the reaction. We assume that the reaction is sufficiently close to the steady state so that $D_{eff}(\epsilon)$ and $\kappa_{eff}(\epsilon)$ can be considered constant over time. This condition is not very restrictive because for many systems D_{eff} and κ_{eff} are essentially constant over several decades (see below). Therefore, for scales larger than ϵ, the area covered by B particles can be regarded as a fractal characterized by dimension $D_{eff}(\epsilon)$ and escape rate $\kappa_{eff}(\epsilon)$.

Let $\epsilon^{(n-1)}(\tau)$ and $\epsilon^{(n)}(0)$ denote the average widths of the stripes right before and right after the nth reaction [3], respectively. Between successive reactions, the stripes shrink due to escape and dissipation as follows: $\epsilon^{(n)}(\tau) = \epsilon^{(n)}(0)e^{-h_{eff}\tau}$, where $h_{eff}=(\kappa_{eff}+\tilde{\kappa})/(2-D_{eff})$ plays the role of an *effective* (contracting) Lyapunov exponent, while $\tilde{\kappa}$ accounts for the nonconservative contribution. When the reaction occurs, the widening due to the reaction is proportional to the reaction range: $\epsilon^{(n+1)}(0)-\epsilon^{(n)}(\tau)\propto\sigma$. The area covered by B particles right before the $(n+1)$th reaction $\mathcal{A}_B^{(n)}$ satisfies $\mathcal{A}_B^{(n)}\propto[\epsilon^{(n)}(\tau)]^{2-D_{eff}}$. These relations can then be combined to yield the following recursive relation for the area: $\mathcal{A}_B^{(n+1)}=e^{-\mu_{eff}}[(\mathcal{A}_B^{(n)})^{1/(2-D_{eff})}+c\sigma]^{2-D_{eff}}$, where $\mu_{eff}=(\kappa_{eff}+\tilde{\kappa})\tau$ and c is a constant geometric factor. From the condition $\mathcal{A}_B^{(n+1)}=\mathcal{A}_B^{(n)}$, our main scaling (3) follows for the area $\mathcal{A}_B$ in the steady state [12]. This scaling holds for both noninertial and inertial particles, regardless of whether the flow is hyperbolic or nonhyperbolic. The hyperbolic case with inertial particles is studied in Ref. [13]. The scaling (3) represents a further step toward generality since it is also valid for nonhyperbolic flows.

To make possible a numerical verification of the scaling law (3), it is necessary at present to use discrete-time maps. To construct a class of maps that captures all essential features of continuous-time chaotic flows, we note the following: (1) the fluid dynamics, determined by $d\mathbf{x}/dt=\mathbf{u}$, is *embedded* in the particle's advection equation and is recovered in the limit $a\rightarrow\infty$; (2) the phase-space contraction is determined by a (irrespective of α); (3) for small inertia, the configuration-space contraction is proportional to $a^{-1}(\alpha-1)$. For an area-preserving map $\mathbf{x}_{n+1}=\mathbf{M}(\mathbf{x}_n)$, representing the dynamics of a time-periodic incompressible fluid, a possible choice for the corresponding *embedding map* representing the *inertial* particle dynamics is $\mathbf{x}_{n+2}-\mathbf{M}(\mathbf{x}_{n+1}) = e^{-a}[\alpha\mathbf{x}_{n+1}-\mathbf{M}(\mathbf{x}_n)]$, where the factors involving a and α are naturally imposed by the particle dynamics [14]. This can be written as

$$\mathbf{x}_{n+1}=\mathbf{M}(\mathbf{x}_n)+\boldsymbol{\delta}_n, \tag{5}$$

$$\boldsymbol{\delta}_{n+1}=e^{-a}[\alpha\mathbf{x}_{n+1}-\mathbf{M}(\mathbf{x}_n)], \tag{6}$$

where $\mathbf{x}$ and $\boldsymbol{\delta}$ can be interpreted as the configuration-space coordinates and the detachment from the fluid velocity, respectively, so that $(\mathbf{x}, \boldsymbol{\delta})$ represents the phase-space coordinates. This class of embedding maps can be a paradigm to address many problems in inertial advection dynamics as it captures the essential properties of Eq. (4). In particular, it is uniformly dissipative, with phase-space contraction rate equal to e^{-2a}; the noninertial dynamics $\mathbf{x}_{n+1}=\mathbf{M}(\mathbf{x}_n)$ is recovered in the limit $a\rightarrow\infty$; and the configuration-space contraction rate is proportional to $e^{-a}(\alpha-1)$ for $e^{-a}(\alpha-1)\ll 1$, in agreement with the distinct behavior expected for aerosols and bubbles. Therefore, for finite a, a rich higher dimensional dynamics with α-dependent $\mathbf{x}$-space projection is expected. Next we consider such a dynamics for both $\alpha>1$ and $\alpha<1$.

To simulate the flow, we consider a two-dimensional area-preserving map that has a pronounced nonhyperbolic character [11]: $(x,y)\rightarrow[\lambda(x-w^2/4),\lambda^{-1}(y+w^2)]$, where $w\equiv x+y/4$ and $\lambda>1$ is the bifurcation parameter. The dynamics is nonhyperbolic for $\lambda\lesssim 6.5$. For $\lambda=4$, for example, there is a major KAM island in the xy space, as shown in Fig. 1(a). Also, from Fig. 1(a), one can see tangencies between the stable and unstable manifolds in the neighborhood of the KAM island, which is a signature of nonhyperbolicity. It is well established that, within the nonhyperbolic region, the dimension of the invariant manifolds is $D=2$ and the escape rate is $\kappa=0$ [10,11]. When this map is embedded in Eqs. (5) and (6), for $\alpha>1$, the xy projection of the resulting four-dimensional map is dissipative in the mixing region (KAM islands and their neighborhoods). In this regime, the dissipation stabilizes marginally stable periodic orbits in the KAM islands of the conservative map, converting the KAM islands and neighborhood into the corresponding basin of attraction of the newly created attractors, as shown in Fig. 1(b). The basin itself extends around the mixing region, mimicking the stable manifold of the conservative dynamics. As a result, the tangencies between the invariant manifolds apparently disappear, suggesting that the advection dynamics of bubble particles is *hyperbolic*. For $\alpha<1$, on the other hand, the configuration-space projection expands in the mixing region and almost all the orbits eventually escape to infinity. However, for small inertia and α close to 1, particles in the regions corresponding to KAM islands of the conservative dynamics and neighborhood are *almost trapped* in the sense that the time it takes to escape is much larger in these regions than outside them. These regions are neglected in our analysis of the open part of the flow, as shown in Fig. 1(c), because filamental structures cannot be resolved inside them.

Numerical simulation of the autocatalytic reaction is performed by dividing the mixing region with a grid where the size of the cells represents the reaction range σ. Particles are placed in the center of the cells. When a reaction takes place in a cell occupied by a B particle, all the cells adjacent to it are *infected* with B particles [15]. We assume that A is the background material and that the reaction takes place simultaneously for all the particles at time intervals τ [16]. If we start with a small seed of B particles near the stable manifold, after a transient time a steady state is reached where B particles are accumulated along a fattened-up copy of the unstable manifold, as shown in Fig. 1(d) for massless point

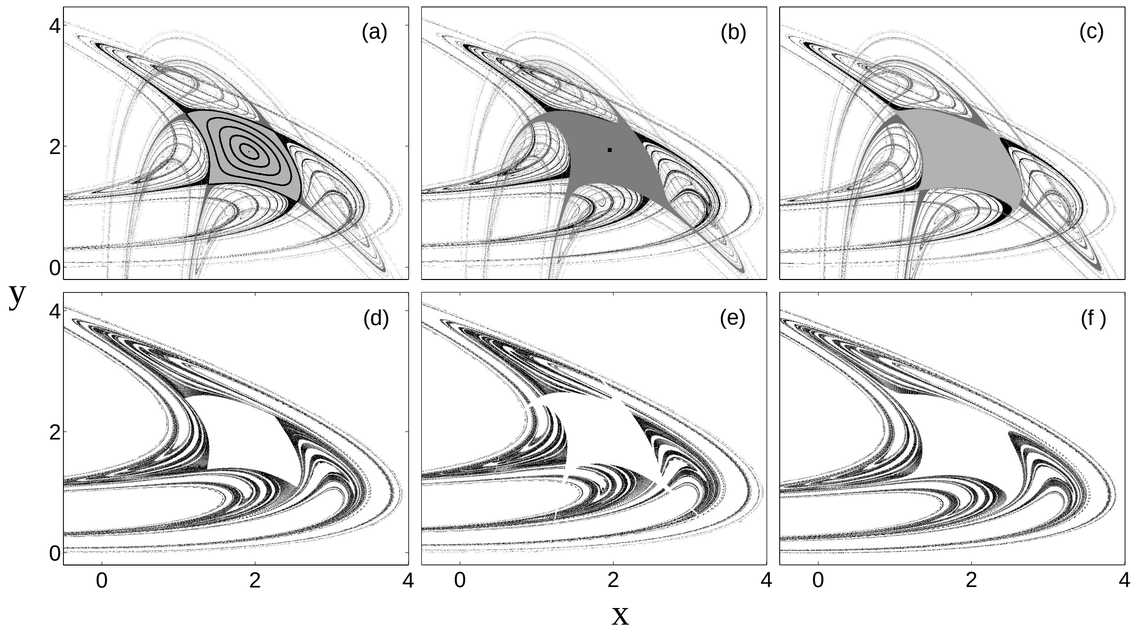

FIG. 1. For $\lambda=4$, (a) KAM island (light gray), and stable (gray) and unstable (black) manifolds for $a=\infty$. (b) Fixed point attractor (black dot), basin of attraction (gray), and unstable manifold (black), for $\alpha=1.05$ and $a=1$. (c) Stable (gray) and unstable (black) manifolds for $\alpha=0.95$ and $a=1$, outside the region covered by the almost trapped orbits (light gray). Particles are launched with initial velocity matching the fluid velocity ($\boldsymbol{\delta}_0=\mathbf{0}$). (d)–(f) Corresponding area covered by B particles in the "open" part of the flow right before the reaction, for $\tau=5$ and $\sigma=5\times10^{-3}$.

particles, in Fig. 1(e) for bubbles, and in Fig. 1(f) for aerosols. In the computation, particles A and B are set to have the same mass ratio and inertia parameters. To compute the effective fractal dimension D_{eff} of the unstable manifold, we use the uncertainty algorithm [17] applied to the first-order approximation of the inverse map. The effective dimension turns out to be constant over many orders of magnitude of variations in ε and it is approximately the same for both noninertial and slightly inertial bubble particles ($D_{eff}=1.73$ for $\varepsilon>10^{-15}$), while it is somewhat smaller for slightly inertial aerosol particles ($D_{eff}=1.68$ for $\varepsilon>10^{-15}$), as shown in Fig. 2(a). Strong evidence of the scaling law (3) is presented in Fig. 2(b) for two different values of the time lag τ, where the scaling exponent is consistent with $D_{eff}=1.73$ for noninertial and bubble particles, and with $D_{eff}=1.68$ for aerosol particles. We see that even though the area $\mathcal{A}_B$ changes with the inertial properties of the particles, the *scaling* of $\mathcal{A}_B$ remains essentially the same for bubbles, as expected from our Cantor-set model.

It is instructive to compare this result with the reaction-free dynamics. The dimension of nonhyerbolic invariant sets can be argued to be integer by mean of a zoom-in technique, where a fast numerical convergence is achieved by focusing on the densest parts of the fractal [11]. The reaction, however, has a *global* character, as it takes place along the unstable manifold around the entire mixing region. This makes the convergence of the relevant effective dimension extremely slow, and that is why the effective dimension is apparently constant.

In summary, we have shown that the dynamical system

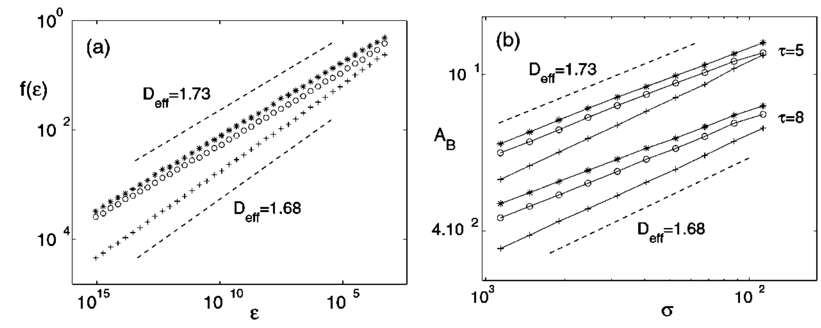

FIG. 2. For $\lambda=4$: (a) Effective dimension of the unstable manifold as computed from the uncertainty method, where $f(\varepsilon)$ is the fraction of ε-uncertain points in the line $x=0$, $0<y<0.1$, of the time-reversed dynamics. (b) Scaling of the relative area $\mathcal{A}_B$ covered by B particles [in the region shown in Figs. 1(d)–(f), right before the reaction] as a function of the reaction range σ for two choices of the time lag τ. In both plots, stars correspond to noninertial particles ($a=\infty$), circles to bubble particles with $\alpha=1.05$ and $a=1$, and plus signs to aerosol particles with $\alpha=0.95$ and $a=1$. The aerosol data in (a) are shifted vertically downward for clarity.

approach to the reactive dynamics in imperfectly mixed flows also applies to realistic situations where nonhyperbolic and inertial effects are relevant. The rate equations of reactive processes are primarily governed by finite-time dynamics and as such change smoothly in the *noninertial*→*inertial* transition, which is in sharp contrast with the metamorphosis undergone by the long-term and asymptotic dynamics of reaction-free particles. We have focused on autocatalytic reactions, but our results are expected to hold whenever the reaction front mimics the underlying unstable manifold and the activity takes place along the boundary of a fattened-up fractal. Examples of this kind of process include infective reactions (e.g., combustion [18]) and collisional reactions in general (e.g., $A+B\rightarrow 2C$, where an unlimited amount of material A is present and material B is continuously injected in the vicinity of the stable manifold [3]). Finally, we observe that our analysis does not rely on the existence of a well-defined fractal set in the advection dynamics. The results remain valid as long as effective values for the fractal dimension and escape rate can be properly defined and are approximately constant over the relevant interval of observation. This is important for environmental processes, whose underlying dynamics is only partially understood [13].

A.E.M. and Y.C.L. were supported by AFOSR through Grant No. F49620-03-1-0290. C.G. was supported by Fapesp and CNPq. A.E.M. thanks Tamas Tél for illuminating discussions.

[1] S. Edouard, B. Legras, F. Lefevre, and R. Eymard, Nature (London) **384**, 444 (1996).

[2] E.R. Abraham, Nature (London) **391**, 577 (1998).

[3] Z. Toroczkai, G. Károlyi, Á. Péntek, T. Tél, and C. Grebogi, Phys. Rev. Lett. **80**, 500 (1998).

[4] See, for example, *Active chaotic flow*, focus issue of Chaos **12**, (2002), and references therein.

[5] Inertial effects on reactive particles have been previously considered for turbulent flows [R. Reigada, F. Sagués, and J.M. Sancho, Phys. Rev. E **64**, 026307 (2001)] and for cellular flows [T. Nishikawa, Z. Toroczkai, C. Grebogi, and T. Tél, *ibid.* **65**, 026216 (2002); Z.H. Liu, Y.-C. Lai, and J.M. Lopez, Chaos **12**, 417 (2002)].

[6] M.R. Maxey and J.J. Riley, Phys. Fluids **26**, 883 (1983).

[7] Equation (4) is an approximation of the Maxey-Riley equation obtained by neglecting the Faxén corrections, the Basset-Boussinesq history force, and the term $[(\mathbf{v}-\mathbf{u})\cdot\nabla]\mathbf{u}$ [A. Babiano, J.H.E. Cartwright, O. Piro, and A. Provenzale, Phys. Rev. Lett. **84**, 5764 (2000)].

[8] I.J. Benczik, Z. Toroczkai, and T. Tél, Phys. Rev. Lett. **89**, 164501 (2002).

[9] M.R. Maxey, Phys. Fluids **30**, 1915 (1987); E. Balkovsky, G. Falkovich, and A. Fouxon, Phys. Rev. Lett. **86**, 2790 (2001).

[10] A.E. Motter and Y.-C. Lai, Phys. Rev. E **65**, 015205 (2002).

[11] Y.-T. Lau, J.M. Finn, and E. Ott, Phys. Rev. Lett. **66**, 978 (1991).

[12] A similar scaling law can be derived in the continuous-time limit $\tau\rightarrow 0$.

[13] T. Tél, T. Nishikawa, A. E. Motter, C. Grebogi, and Z. Toroczkai (unpublished).

[14] For $\alpha=1$, this equation reduces to the first-order approximation of the bailout embedding map introduced by [J.H.E. Cartwright, M.O. Magnasco, and O. Piro, Phys. Rev. E **65**, 045203 (2002)] to study the advection dynamics of neutrally buoyant particles.

[15] For numerical convenience, the autocatalytic reaction is followed by coalescence, so that when more than one B particle is found in the same cell, they are all replaced by a single B particle in the center of the cell. Without coalescence, the number of B particles diverges because of the shrinking due to dissipation, but the area $\mathcal{A}_B$ still reaches a steady state. Since we focus on the *area* covered by B particles, our results do not depend on the coalescence.

[16] The time lag τ is assumed to be on the order of or smaller than the relevant time scale of the advection dynamics $\tau_f=1/\kappa_{eff}(\sigma)$. For $\tau\gg\tau_f$, the reaction undergoes an emptying transition and the Cantori structures near the KAM tori cannot be neglected. In this regime, almost all the particles along the unstable manifold escape between successive reactions, and the hypothesis that reagent B is distributed along approximately uniform stripes breaks down outside the Cantori. However, since Cantori are obstacles to the transport of particles, for small enough σ, a high concentration of particles can still be found inside the hierarchy of Cantori structures. For details we refer to A. P. S. de Moura and C. Grebogi (unpublished).

[17] C. Grebogi, S.W. McDonald, E. Ott, and J.A. Yorke, Phys. Lett. **99A**, 415 (1983).

[18] I.Z. Kiss, J.H. Merkin, S.K. Scott, P.L. Simon, S. Kalliadasis, and Z. Neufeld, Physica D **176**, 67 (2003).